

1 Article type: Rapid Report

2 **Divergence in red light responses associated with thermal reversion of**
3 ***PHYTOCHROME B* between high- and low-latitude species**

4

5 Hajime Ikeda^{*},¹, Tomomi Suzuki², Yoshito Oka², A. Lovisa S. Gustafsson³, Christian
6 Brochmann³, Nobuyoshi Mochizuki², Akira Nagatani²

7 ¹ Institute of Plant Science and Resources, Okayama University, 2-20-1 Chuo, Kurashiki,
8 Okayama 710-0046, Japan

9 ² Graduate School of Science, Kyoto University, Kitashirakawa-Oiwake, Sakyo, Kyoto
10 606-8502, Japan

11 ³ Natural History Museum, University of Oslo, PO Box 1172 Blindern, NO-0318 Oslo,
12 Norway

13 **Corresponding Author: Hajime Ikeda**

14 Institute of Plant Science and Resources, Okayama University, 2-20-1 Chuo, Kurashiki,
15 Okayama 710-0046, Japan

16 TEL: +81-86-434-1238/FAX: +81-86-434-1249 E-mail: ike@okayama-u.ac.jp

17 **Orchid IDs**

18 Hajime Ikeda: <https://orcid.org/0000-0002-3014-3585>

19 Yoshito Oka: <https://orcid.org/0000-0002-6703-9853>

20 A. Lovisa S. Gustafsson: <https://orcid.org/0000-0001-8819-7562>

21 Christian Brochmann: <https://orcid.org/0000-0002-8906-7273>

22

23 **Brief heading:** Evolution in red light responses between high- and low-latitude species

24 Total words: 4031 words

25 (Introduction: 656, Materials and Methods: 1627, Results: 1111, Discussion: 637)

26 Figures: 4 (Color figures: Fig. 1, 2, 3, and 4)

27 Tables: 0

28 Supporting information: 11

29

30 **Summary**

- 31 ● Phytochromes play a central role in mediating adaptive responses to light and
32 temperature throughout plant life cycles. Despite evidence for adaptive importance
33 of natural variation in phytochromes, little is known about molecular mechanisms
34 that modulate physiological responses of phytochromes in nature.
- 35 ● We show evolutionary divergence in physiological responses relevant to thermal
36 stability of a physiologically active form of phytochrome (Pfr) between two sister
37 species of Brassicaceae growing at different latitudes.
- 38 ● The higher-latitude species (*Cardamine bellidifolia*; *Cb*) responded more strongly to
39 light limited condition than its lower-latitude sister (*C. nipponica*; *Cn*). Moreover,
40 *CbPHYB* conferred stronger responses to both light limited and warm conditions in
41 the *phyB*-deficient mutant of *Arabidopsis thaliana* than *CnPHYB*: i.e., Pfr CbphyB
42 was more stable in nuclei than CnphyB.
- 43 ● Our findings suggest that fine-tuning Pfr stability is a fundamental mechanism for
44 plants to optimise phytochrome-related traits in their evolution and adapt to spatially
45 varying environments, and open a new avenue to understand molecular mechanisms
46 that fine-tune phytochrome responses in nature.

47 Keywords: alpine plants; Brassicaceae; *Cardamine*; phytochrome; thermal
48 reversion.

49

50 **Introduction**

51 Sensing ambient environments and subsequent physiological changes are crucial for
52 survival and reproductive success of plants. Phytochromes, which are red- (R) and far-
53 red (FR) light receptors, play a central role in physiological responses to light conditions
54 throughout plant life cycles, including germination, seedling growth and flowering (Jiao
55 *et al.*, 2007). Recently, phytochromes have also been identified as a thermal sensor as
56 well (Jung *et al.*, 2016; Legris *et al.*, 2016), and therefore mediate physiological responses
57 by integrating both light and temperature signals (Legris *et al.*, 2017; Casal & Questa,
58 2018). Seed plants have multiple phytochromes, of which three discrete classes of
59 apoprotein-encoding genes (*PHYA–PHYC*) are conserved in angiosperms (Mathews,
60 2010). In the model plant *Arabidopsis thaliana*, five phytochromes (phyA–phyE) have
61 been identified (Sharrock & Quail, 1989; Clack *et al.*, 1994). PhyA and phyB play
62 prominent roles (Franklin & Quail, 2010), whereas phyC–phyE have redundant (Franklin
63 *et al.*, 2003) but physiologically important roles in specific environments, including at
64 low temperatures.

65 Molecular evolutionary analyses have detected a signature of divergent selection in *PHYA*
66 of *Arabidopsis lyrata* (Toivainen *et al.*, 2014) and in *PHYE* of two alpine species,
67 *Cardamine nipponica* (Ikeda *et al.*, 2009) and *Arctericia nana* (Ikeda & Setoguchi, 2010),
68 of which plants growing at different latitudes have alleles encoding different amino acid
69 sequences. In addition, amino acid replacements in *PHYB2* of *Populus tremula* are
70 associated with latitudinal variation in its bud set timing, which is an ecologically
71 important trait (Ingvarsson *et al.*, 2006; Ingvarsson *et al.*, 2008). Although these studies
72 did not demonstrate functional differences conferred by alternative alleles with amino
73 acid changes, other studies of *A. thaliana* have shown that natural variation in amino acid
74 sequences changes the light sensitivity of phytochromes; accessions from higher latitude
75 had more light sensitive phytochromes [phyB (Filiault *et al.*, 2008) and phyC
76 (Balasubramanian *et al.*, 2006)] than those from lower latitude. Furthermore, a recent
77 study demonstrated that enhanced phyA activity in *Cardamine hirsuta* is responsible for
78 its shade tolerance (Molina-Contreras *et al.*, 2019). Collectively, these studies suggest
79 that modulating the light sensitivity of phytochromes as well as their physiological
80 activity may be important in adaptation to spatially (in particular latitudinally) varying

81 environments.

82 Phytochromes are synthesized in physiological inactive form (Pr). Pr absorbs R light and
83 changes its conformation to physiologically active one (Pfr), whereas Pfr absorbs FR light
84 and returns to Pr. In addition, prolonged darkness and/or warmer conditions even in R
85 light promotes reversion of Pfr to Pr [dark or thermal reversion (Legris *et al.*, 2016)].
86 Upon R light irradiation, phyB accumulates in the nucleus and forms nuclear bodies
87 (NBs; Yamaguchi *et al.*, 1999; Chen *et al.*, 2003), which stabilize Pfr as well as its
88 physiological activity even in prolonged darkness (Van Buskirk *et al.*, 2014). Given that
89 amino acid changes can influence thermal stability of phyB Pfr (Kretsch *et al.*, 2000; Oka
90 *et al.*, 2004; Oka *et al.*, 2008; Zhang *et al.*, 2013), fine-tuning of Pfr thermal stability
91 might represent the evolutionary mechanism underlying divergent selection on
92 phytochrome genes as well as the differential light sensitivity of phytochromes. However,
93 there is neither evidence of natural variation in Pfr thermal stability (Legris *et al.*, 2017)
94 nor evidence for evolutionary importance of fine-tuning Pfr stability (Enderle *et al.*, 2017).
95 In this study, we assess evolutionary divergence in phytochrome-related phenotypes
96 between two sister species of perennial herbs in Brassicaceae, *Cardamine bellidifolia*
97 (*Cb*) and *Cardamine nipponica* (*Cn*) (Ikeda *et al.*, 2012); the former occurs in the
98 circumarctic region as well as in the alpine regions of North America and East Asia and
99 the latter is endemic to high mountains in the Japanese Archipelago (Fig. 1a). We show
100 that these sister species growing at different latitude have phyB with different Pfr thermal
101 stability; the lower-latitude *C. nipponica* has more thermal-sensitive phyB than the
102 higher-latitude *C. bellidifolia*. Our findings suggest that fine-tuning Pfr thermal stability
103 is one of molecular mechanisms for adapting to environments with different light and
104 temperature conditions.

105 **Materials and Methods**

106 **Seedling assays**

107 Seeds of three accessions of each of *C. bellidifolia* and *C. nipponica* (Table S1), which
108 were grown for five or more generations of selfing after initially collected from natural
109 populations, were embedded on rockwool and irradiated with continuous light by 3-in-1
110 LED (ca. 70 $\mu\text{mol m}^{-2} \text{sec}^{-1}$; ca. 26, 14, 30 $\mu\text{mol m}^{-2} \text{sec}^{-1}$ with peak wave length at 445,
111 520, 660 nm, respectively). After the root emerged, seedlings were grown in one of four
112 light conditions for seven days at 22 °C: cR, continuous R light with different intensity

113 (ca. 10, 30, and 150 $\mu\text{mol m}^{-2} \text{sec}^{-1}$ with peak wave length at 660 nm); pR, 15 min R light
114 pulses (ca. 150 $\mu\text{mol m}^{-2} \text{sec}^{-1}$ with peak wave length at 660 nm) every 12 hr darkness;
115 pR+FR, pR followed by 15 min FR light pulses (ca. 100 $\mu\text{mol m}^{-2} \text{sec}^{-1}$ with peak wave
116 length at 730 nm) every 12 hr darkness; cD, continuous darkness (cD).

117 Seeds of *A. thaliana* were surface-sterilized and sown on 0.8% agar plates containing
118 Murashige-Skoog (MS) medium without sucrose. In addition to transgenic plants
119 overexpressing *PHYB* of *C. bellidifolia* and *C. nipponica* (see below), we also used
120 Landsberg *erecta* (*Ler*), phyB-5 mutation (Reed 1993), and transgenic *A. thaliana*
121 expressing *PHYB* under the control of the authentic *PHYB* promoter (Bpro7 in Endo *et*
122 *al.*, 2005) and under the 35S promoter (PBG in Yamaguchi *et al.*, 1999). The plates were
123 kept in darkness at 4°C for five days and then moved to cR (ca. 30 $\mu\text{mol m}^{-2} \text{sec}^{-1}$ with
124 peak wave length at 660 nm) at 22°C. After one day in cR, seedlings were grown in cR,
125 pR at specific intervals of darkness (8, 12, or 16 hr), pR+FR or cD for five days at 16, 22,
126 and 28°C.

127 Seedlings were photographed and their hypocotyl lengths were measured using ImageJ
128 (<https://imagej.nih.gov/ij/>). The hypocotyl length was analyzed with a generalized linear
129 mixed model (GLMM) using the glmer function from the package LME4 (Bates *et al.*,
130 2015) in R v3.2.3. For *Cardamine* seedlings, the effects of the light intensity (0, 10, 30,
131 and 150 $\mu\text{mol m}^{-2} \text{sec}^{-1}$) or pR (pR, pR+FR and cD) and species (*C. bellidifolia* and *C.*
132 *nipponica*) on hypocotyl length were examined by a model specifying independent
133 accessions of each species [Ava, Den, and Yuk (*C. bellidifolia*); Dai, Kis, and Shi (*C.*
134 *nipponica*)] as a random effect on the species. After optimization, Gamma distribution
135 with log link and Gaussian distribution with log link was applied for the analyses of light
136 intensity and pR, respectively. For *A. thaliana* transgenic seedlings, the effects of light
137 (cR, cD and pR) or temperature (16, 22 and 28°C) and *PHYB* allele (*CbPHYB* and
138 *CnPHYB*) on hypocotyl length were examined by a model specifying three replicate
139 transgenic lines of each *PHYB* as a random effect. After optimization, Gamma distribution
140 with log or inverse link was applied.

141 **Sequence analyses of phytochrome genes**

142 DNA of *C. bellidifolia* and *C. nipponica* were extracted from silica-dried leaves that were
143 collected from the natural populations or extracted in the previous study (Ikeda *et al.*,
144 2008), and sequences of phytochrome genes were determined following the previous

145 study (Ikeda *et al.*, 2009). Together with the previously published sequences from 11
146 individuals (Ikeda *et al.*, 2009; Ikeda *et al.*, 2011), 16 individuals of each species were
147 included in this study (Table S1). All new sequences of phytochrome genes were
148 deposited in DDBJ (Table S1). After haplotype sequences of each gene were determined
149 by Bayesian method implementing PHASE (Stephens & Donnelly, 2003), McDonald-
150 Kreitman (MK) test was conducted to compare the number of synonymous and
151 nonsynonymous substitutions of both fixed differences between the species and
152 polymorphisms within species using DnaSP.

153 **Molecular evolutionary analyses of *PHYB***

154 *PHYB* gene trees were estimated based on both amino acid and nucleotide sequences. In
155 addition to *C. bellidifolia* and *C. nipponica*, 21 species of Brassicaceae were included in
156 the analyses (Table S2). The nucleotide sequences were determined in the present study
157 for three additional *Cardamine* species (*C. alpina*, *C. resedifolia*, and *C. glauca*) and
158 coding DNA sequences (CDS) of *PHYB* were obtained from published genome data for
159 the remaining species. Amino acid sequences were determined from the nucleotide
160 sequences. After the amino acid and nucleotide sequences had been separately aligned
161 using Clustal W (Edgar, 2004) implemented by MEGA7, the substitution model of amino
162 acid (JTT+G+I) and nucleotide (HKY+G+I) sequences was selected based on Bayesian
163 information criteria using Prottest v3.4 (Darriba *et al.*, 2011) and jModelTest v2.1
164 (Darriba *et al.*, 2012), respectively. Trees were estimated by maximum likelihood (ML)
165 using PhyML (Guindon *et al.*, 2010) with the SPR tree search option and by Bayesian
166 method using MrBayes 3.1.2 (Ronquist & Huelsenbeck, 2003). Branch support was
167 evaluated with 1,000 bootstrap resamplings for ML and posterior probability for Bayesian
168 trees. Following a previous phylogenetic study (Kagale *et al.*, 2014), trees were rooted
169 using *Aethionema arabicum* as the outgroup.

170 In addition, we analysed the ratio of nonsynonymous to synonymous substitutions ($\omega =$
171 d_N/d_S) using CODEML in PAML4.7 (Yang, 2007). By assuming a branch model (Yang
172 & Nielsen, 1998), where unique ω was applied for either *C. bellidifolia* or *C. nipponica*,
173 the likelihood of the branch model was compared with a null model assuming a single ω
174 (M0a). The nucleotide sequences corresponding to the most basal amino acid sequences
175 in each of *C. bellidifolia* and *C. nipponica* were used for the analyses. Highly supported
176 clades (bootstrap > 90 and posterior probability > 0.95 in either amino acid or nucleotide

177 trees) were applied for the initial topology for the analyses. The convergence of likelihood
178 and ω was evaluated by repeated analyses with different initial values ($\omega = 0, 1, \text{ and } 10$).

179 **Plasmid construction and plant transformation**

180 Total RNA of *C. bellidifolia* (Ava) and *C. nipponica* (Kis), accessions with the most
181 common sequence of PHYB in each species, was extracted from leaves of cultivated
182 plants using the RNeasy Kit (Qiagen, Hilden, Germany) and used for synthesizing cDNA.
183 The entire coding region of *CbPHYB* and *CnPHYB* was amplified from cDNA by PCR
184 using PrimeSTAR Max Premix (Takara BIO, Otsu, Japan) with a primer pair (Forward:
185 CACGGGGGACTCTAGAATGGTTTCCGGAGGCGGCGGA, Reverse:
186 TGCTCACCATGTCGACATATGGCATCATCAACATCATAT). After a transformation
187 vector P35S:P2G (Kong *et al.*, 2006), which cloned PHOT2-GFP into pPZP211/*P_{35S}-nosT*,
188 was cut by *Xba*I and *Sal*I to remove *PHOT2*, the amplified *CbPHYB* or *CnPHYB* was
189 inserted into the vector using InFusion (Clontech, Mountain View, CA, USA). The *phyB*-
190 5 mutant (Accession, Landsberg *erecta*; Reed *et al.*, 1993) was transformed by
191 *Agrobacterium tumefaciens* mediated by the floral dip method (Clough & Bent, 1998),
192 and homozygous transgenic lines were selected following the previous procedure (Oka *et*
193 *al.*, 2004).

194 **Immunoblot assays of PHYB**

195 Total protein was extracted from ca. 35 mg seedling material of the transgenic plants with
196 *CbPHYB-GFP* or *CnPHYB-GFP* using extraction buffer (APRO Science, Tokushima,
197 Japan) and used for SDS-PAGE, protein blotting, and immunodetection following the
198 previous procedure (Oka *et al.*, 2004). Using anti-GFP monoclonal antibody (Nacalai
199 Tesque, Kyoto, Japan) and anti-Actin polyclonal antibody (Abcam, Cambridge, MA), the
200 relative level of PHYB-GFP to Actin was quantified with Clarity Western ECL Substrate
201 (Bio-Rad) using LAS-4000 (GE Healthcare). Three independent samples were used for
202 replicated measurements.

203 **Subcellular localization of PHYB**

204 Seedlings of transgenic *A. thaliana* were grown on 0.8% agar plates containing MS
205 medium without sucrose in cR (ca. $10 \mu\text{mol m}^{-2} \text{sec}^{-1}$) at 22 °C. The green fluorescent
206 protein (GFP) in nuclei of hypocotyl epidermal cells in two-day old seedlings was
207 mounted on the stage under a dim green safelight and observed with a confocal laser
208 microscope (Olympus) before and after 12 hr darkness. Single scanned images of each

209 seedling immediately after preparation were used for the NB measurement. The size of
210 NBs were measured using ImageJ. The effects of *PHYB* allele (*CbPHYB* and *CnPHYB*)
211 and 12 hr darkness on NB sizes were examined by a generalized linear mixed model
212 (GLMM) with three replicate transgenic lines of each *PHYB* as a random effect. Gamma
213 distribution with log link was applied for the analysis.

214 ***In vitro* assay of thermal reversion**

215 *In vitro* thermal stability of Pfr was assessed using the N-terminal 651 amino acid
216 fragment (N651) of CbPHYB and CnPHYB. The N651 of *C. bellidifolia* and *C.*
217 *nipponica* were amplified from the above synthesized cDNA by PCR using PrimeSTAR
218 Max Premix (Takara BIO) with a primer pair (Forward:
219 GGCAAAGCACCCGGGATATGGCATCATCAACATCATAT, Reverse:
220 CTTGGCAAAGCACCCCTGCACCTAGCTCATCA) and were inserted into the pTYB2
221 vector (New England Biolabs, Beverly, MA) using InFusion (Clontech, Mountain View,
222 CA). *Escherichia coli* strain BL21 (New England Biolabs) was transformed by the
223 plasmids and cultured in 2 L of LB medium containing 50 $\mu\text{g mL}^{-1}$ of carbenicillin for
224 20 hr at 28 °C until the cell density reached $A_{600} = 0.8$. Afterwards, 0.4 mM isopropyl-
225 thio-B-D-galactoside was added, and the media were further cultured for 16 hr at 16 °C.
226 Proteins were extracted from lysed cells using sonication, purified with the IMPACT kit
227 (New England BioLabs) and eluted by self-cleaved in the presence of 40 mM 1,4-
228 dithiothreitol for two days at 4 °C.

229 The purified protein was mixed with 5 μM phycocyanobillin (Oka *et al.* 2004) and used
230 for measurement of absorption with a UV-1600PC spectrophotometer (Shimadzu,
231 Kyoto, Japan) at 27 °C. The baseline of each observation was recorded after irradiation
232 with FR light for 5 min. After 3 min irradiation of R light, absorbance between 525 and
233 800 nm was repeatedly measured every 10 min for 60 min. Relative amounts of Pfr
234 ($\text{Pfr}/\text{P}_{\text{total}}$) were calculated based on differences in the absorption peaks at red (648 nm)
235 and far-red (709 nm) light, where the difference immediately after the R light irradiation
236 was set as $\text{Pfr}/\text{P}_{\text{total}} = 1$. The effects of *PHYB* allele (*CbPHYB* and *CnPHYB*) and
237 duration of darkness on $\text{Pfr}/\text{P}_{\text{total}}$ were examined by a generalized linear mixed model
238 (GLMM) with repeated measurement as random effects. After optimization, Gaussian

239 distribution with log link was applied for the analysis.

240 **Results**

241 **Red light response differed between *Cardamine bellidifolia* and *C. nipponica***

242 Given that light sensitivity of phytochromes has been reflected in hypocotyl growth of
243 seedlings under R light in *A. thaliana* (Maloof *et al.*, 2001; Balasubramanian *et al.*, 2006;
244 Filiault *et al.*, 2008), we measured hypocotyl lengths of *C. bellidifolia* and *C. nipponica*
245 grown in cR. Hypocotyl lengths differed significantly between the two species in weaker
246 R light (10 and 30 $\mu\text{mol m}^{-2} \text{sec}^{-1}$) at 22 °C (Fig. 1b, c and Fig. S1; $P < 0.001$), whereas
247 the two species had similar hypocotyl lengths in cD ($P = 0.66$) and strong R light (150
248 $\mu\text{mol m}^{-2} \text{sec}^{-1}$, $P = 0.24$), suggesting that *C. bellidifolia* and *C. nipponica* differ in their
249 light sensitivity at R light limited conditions.

250 Pulse of R light at 12 hr intervals (pR) was much less effective than cR to inhibit the
251 hypocotyl growth (Fig. 1b, d). Notably, the response to pR differed significantly between
252 the two species at 22 °C [generalized linear mixed model (GLMM): Light \times Species: $P <$
253 0.0001], with *C. nipponica* having longer hypocotyls in pR than *C. bellidifolia* (Fig. 1b,
254 d: $P < 0.0001$). Pulse of FR light following pR diminished the repressive effects of
255 hypocotyl growth in pR (pR vs. pR+FR: *Cb*, $P < 0.0001$; *Cn*, $P < 0.001$), resulting in
256 similar hypocotyl lengths with cD (Fig. 1b, d, *Cb*, $P = 0.18$; *Cn*, $P = 0.28$). These
257 observations suggest that the higher-latitude *C. bellidifolia* is more sensitive to R light
258 and persist stronger phytochrome signals in darkness than the lower-latitude *C. nipponica*.

259 ***CnPHYB* was exclusively divergent between the two species**

260 One of possible explanation for the above observations is that Pfr in the higher-latitude
261 *C. bellidifolia* was more stable than that in the lower-latitude *C. nipponica*. To explore
262 whether phytochromes are responsible for the difference in seedling responses to R light,
263 we investigated molecular evolution of four phytochrome genes (*PHYA*–*PHYC*, and
264 *PHYE*) across range-wide samples of *C. bellidifolia* and *C. nipponica* (Fig. 1a, Table S1).
265 Although all analysed genes exhibited similar level of divergence between species ($K =$
266 0.0033–0.0040; Table S2), *PHYB* and *PHYE* exhibited a non-neutral pattern of
267 synonymous and nonsynonymous substitutions (Fig. 2a). *PHYB* showed the highest
268 number of fixed amino acid differences between the two species, whereas *PHYE* showed
269 excess of nonsynonymous polymorphisms within species. Notably, fixed nonsynonymous

270 substitutions between these species were exclusively found in *PHYB* (Fig. 2a).
271 To better understand the evolutionary history of *PHYB*, we constructed gene trees
272 including 21 Brassicaceae species (Table S3) using both amino acid and nucleotide
273 sequences. Consistent with previous phylogenetic inference (Ikeda *et al.*, 2012), both
274 maximum likelihood and Bayesian trees resolved a reciprocally monophyletic
275 relationship between *C. bellidifolia* and *C. nipponica* [Fig. 2b, S2; bootstrap values = 74
276 (amino acids) and 100 (nucleotides), posterior probabilities = 1.00 (both amino acids and
277 nucleotides)]. The divergence of *CnPHYB* had higher ratio of nonsynonymous to
278 synonymous substitutions ($\omega = 1.29$) than the remaining branches ($\omega = 0.07$, $P < 0.01$;
279 Fig. 2b), whereas such accelerated evolution was not detected in the divergence of
280 *CbPHYB* ($\omega = 0.32$, $P = 0.13$; Fig. 2b). Consistent with the higher evolutionary rate in
281 *CnPHYB*, five of seven amino acid replacements were uniquely found in *C. nipponica*
282 (Fig. 2c). In contrast, only one polymorphism (S495T) was shared among other species
283 and one polymorphism (S594C) was uniquely found in *C. bellidifolia* (Fig. 2c and S3).

284 **CbphyB was more sensitive to red light than CnphyB**

285 As expected from thermal reversion of Pfr in darkness, pR with longer intervals of
286 darkness resulted in longer hypocotyls in *A. thaliana* (Fig. S4). This hypocotyl response
287 in pR was completely impaired in the *phyB*-deficient mutant, whereas these phenotypes
288 in the mutants were strongly complemented in transgenics expressing *PHYB* of *A.*
289 *thaliana* fused to GFP under control of either the *A. thaliana* *PHYB* promoter
290 (*PHYB_{pro}::PHYB-GFP*) or the 35S promoter (*35S_{pro}::PHYB-GFP*; Fig. S4).

291 Transgenics overexpressing *CbPHYB* and *CnPHYB* showed little difference in hypocotyl
292 length in cD at 22 °C (Fig. 3b; $P = 0.50$). In contrast, the response to the light differed
293 between *CbPHYB* and *CnPHYB* (Fig. 3b). *CbPHYB* conferred significantly shorter
294 hypocotyls in cR and pR than *CnPHYB* (Fig. 3c; $P < 0.001$ and $P < 0.0001$ for cR and
295 pR, respectively), where responses to light conditions differed between *CbPHYB* and
296 *CnPHYB* (GLMM: Light \times *PHYB*: $P < 0.0001$). Notably, CnphyB Pfr was more stable
297 in the transgenics than in *C. nipponica*, whose hypocotyls in pR have similar length as
298 those in cD (Fig. 1), plausibly reflecting enhanced phyB Pfr activity due to overexpression.
299 Immunoblot assays showed that there was no difference between CnphyB and CbphyB
300 levels after 12 hr darkness (Fig. S5). Given that the polymorphisms in phyB barely
301 influenced the sensitivity of antibody to detect GFP, degradation of phyB unlikely

302 explained the phenotypic difference in pR. In contrast, the difference in pR was
303 diminished in pR+FR (Fig. 3; $P = 0.11$), resulting in hypocotyl length similar to with
304 those in cD (*CbPHYB*, $P = 0.21$; *CnPHYB*, $P = 0.55$). Taken together, the hypocotyl
305 response to pR could be attributed to the thermal stability of Pfr in darkness rather than
306 protein levels. Furthermore, the size of nuclear bodies decreased more in *CnphyB* than
307 *CbphyB* after 12 hr darkness (Fig. 3d, e; $P < 0.001$), directly supporting that *CbphyB* Pfr
308 was more stable than *CnphyB* Pfr *in vivo*: *CbphyB* is extraordinarily stable compared to
309 *CnphyB*, which was comparable to *AtphyB* (Van Buskirk *et al.*, 2014). However, the
310 thermal stability of phyB Pfr *in vitro* was inconsistent with the observation *in vivo*: the
311 *CbphyB* Pfr decreased more rapidly than *CnphyB* (Fig. S6; $P < 0.001$).

312 ***CbphyB* is less sensitive to higher temperatures than *CnphyB***

313 Consistent with the faster thermal reversion of phyB in warmer conditions (Jung *et al.*,
314 2016; Legris *et al.*, 2016), phyB inhibited the hypocotyl elongation in *A. thaliana* more
315 at lower temperatures in cR (Fig. S7). Transgenics overexpressing *CbPHYB* and *CnPHYB*
316 showed little difference in hypocotyl length in cD (Fig. 4a; $P > 0.05$) as well as at 16°C
317 in cR (Fig. 4; $P = 0.47$). In contrast, the response to temperature significantly differed
318 between *CbPHYB* and *CnPHYB* (Fig. 4; GLMM: Temperature \times Light \times *PHYB*: $P <$
319 0.0001). *CnPHYB* conferred longer hypocotyls than *CbPHYB* exclusively at higher
320 temperatures in cR (Fig. 4; $P < 0.0001$ and $P < 0.0001$ for 22°C and 28°C, respectively).
321 In addition, *CnPHYB* conferred more sensitive responses to higher temperature than
322 *CbPHYB* in pR (Fig. 4). Hence, as expected from the thermal stability, our results suggest
323 that phyB in *C. bellidifolia* is less sensitive to high temperatures than phyB in *C.*
324 *nipponica*.

325 **Discussion**

326 Light sensitivity of phytochromes is an important mechanism for plants to adapt to
327 environments varying along latitude; plants growing in higher latitude have
328 phytochromes with higher light sensitivity (Balasubramanian *et al.*, 2006; Filaault *et al.*,
329 2008). Together with the finding of difference in light sensitivity of phytochrome between
330 two sister species growing at different latitude (Fig. 1), our study demonstrates that the
331 lower-latitude *Cardamine nipponica* has phyB with lower light sensitivity probably due
332 to less thermal stability of Pfr *in vivo* than the higher-latitude *C. bellidifolia* (Figs. 3, 4).
333 Collectively, this study provides the first evidence of evolutionary divergence in Pfr

334 thermal stability of phyB between species or accessions, suggesting that fine-tuning Pfr
335 stability is one of the molecular mechanisms in plants to modify light or temperature
336 sensitivity of phytochromes and optimise phytochrome-related traits in nature. Given that
337 higher thermal-stable Pfr confers shorter hypocotyls even in cR light (Fig. 4), Pfr stability
338 may be associated with the previously observed latitudinal difference in light sensitivity
339 of phytochromes in *A. thaliana* (Balasubramanian *et al.*, 2006; Filiault *et al.*, 2008).
340 Although amino acid polymorphisms in the two *Cardamine* species were not shared
341 among species in Brassicaceae (Fig. 2), fine-tuning Pfr stability might be a common
342 mechanism underlying latitudinal adaptation.

343 Since *C. nipponica* grows under shorter photoperiods and higher temperature in summer
344 (Fig. S8), it may frequently experience either higher temperatures in certain periods of
345 days or larger diurnal temperature changes compared to *C. bellidifolia*, which grows in
346 cooler temperature with less diurnal changes. Faster decline of phytochrome activity at
347 higher temperatures might be beneficial under the temperature regime of *C. nipponica*,
348 whose phytochrome activity was mostly diminished in 12 hr darkness (Fig. 1).
349 Nevertheless, the present study exclusively focused on the hypocotyl response to R light
350 in *C. bellidifolia* and *C. nipponica* (Fig. 1), and thus could clarify neither their difference
351 in temperature responses nor the ecological importance of their difference in the Pfr
352 stability. Given their genetic distinctiveness (Ikeda *et al.*, 2012), *C. bellidifolia* and *C.*
353 *nipponica* may have numerous genetic differences in their physiological traits including
354 light and temperature responses. Further studies are required to assess their ecological
355 divergence as well as selective forces associated with the phyB Pfr stability.

356 It should be noted that our study did not fully elucidated molecular mechanisms that fine-
357 tune Pfr stability. Since we investigated phytochrome responses in an identical genetic
358 background, molecular properties of CbphyB and CnphyB could be responsible for the
359 difference in hypocotyl responses of transgenics. Previous studies show that mutations on
360 the PHY domain either weakened (G564A, S584F, A587T; Oka *et al.*, 2004; Oka *et al.*,
361 2008) or enhanced (G564E; Kretsch *et al.*, 2000) phyB Pfr stability consistently both *in*
362 *vitro* and *in vivo*, and hence the three amino acid changes on the PHY domain (Fig. S3)
363 might be responsible for the difference in Pfr stability between CbphyB and CnphyB.
364 However, our *in vitro* assay did not support this hypothesis: i.e., *in vitro* Pfr stability of
365 the N651 of CbphyB and CnphyB (Fig. S6) was discordant with Pfr stability *in vivo* (Fig.

366 3) as well as hypocotyl responses in the two *Cardamine* species (Fig. 1) and the
367 transgenics (Fig. 3). Given that the C-terminal of phyB is essential for dimerization and
368 accelerates thermal reversion (Burgie *et al.*, 2017), the present study may not be sufficient
369 to evaluate *in vitro* thermal stability of full-length CbphyB and CnphyB. Furthermore, Pfr
370 thermal stability *in vivo* is determined not only by phytochrome itself but also by
371 interaction with chromophore (Burgie *et al.*, 2017) or other proteins, including
372 PHOTOPERIODIC CONTROL OF HYPOCOTYL 1 (PCH1; Enderle *et al.*, 2017; Huang
373 *et al.*, 2019), PCH1-LIKE (PCHL; Enderle *et al.*, 2017) and *Arabidopsis* response
374 regulator 4 (ARR4; Sweere *et al.*, 2001). Addressing these issues is required for
375 understanding molecular mechanisms that fine-tune phytochrome responses in nature.

376 **Acknowledgments**

377 We thank Rieko Kobashi and Daisuke Saisho for assisting with experiments, Hiroaki
378 Setoguchi, Hiroyuki Higashi and Valentin Yakubov for assistance to collect samples,
379 Hirokazu Tsukaya for advice on cultivation of *Cardamine* species, Kojiro Takanashi and
380 Takashi Hirayama for suggestions on physiological experiments, Gen Sakurai for
381 suggestions on statistical analyses, and anonymous reviewers for constructive comments
382 and suggestions on the manuscript. This work was supported by JSPS KAKENHI (Grant
383 Number 23657015, 20K06798), the Yakumo Foundation, the Wesco Foundation and the
384 Inamori Foundation.

385 **Author Contributions**

386 H.I. designed the research and experiments, collected plant materials, performed all
387 experiments and data analyses, interpreting data and wrote the draft of the manuscript;
388 T.S. made transgenic *A. thaliana*; L.G. and C.B. collected plant materials; Y.O. and N.M.;
389 A.N. designed experiments and interpreted data; all authors discussed and commented on
390 the manuscript.

391 **Reference**

392

- 393 **Balasubramanian S, Sureshkumar S, Agrawal M, Michael TP, Wessinger C, Maloof JN,**
394 **Clark R, Warthmann N, Chory J, Weigel D. 2006.** The PHYTOCHROME C
395 photoreceptor gene mediates natural variation in flowering and growth responses of
396 *Arabidopsis thaliana*. *Nat Genet* **38**(6): 711-715.
397 **Bates D, Mächler M, Bolker B, Walker S. 2015.** Fitting linear mixed-effects models using lme4.
398 *Journal of Statistical Software* **67**(1): 1–48.
399 **Burgie ES, Bussell AN, Lye SH, Wang T, Hu W, McLoughlin KE, Weber EL, Li H, Vierstra**
400 **RD. 2017.** Photosensing and thermosensing by Phytochrome B require both proximal and

401 distal allosteric features within the dimeric photoreceptor. *Sci Rep* 7(1): 13648.

402 **Casal JJ, Questa JI. 2018.** Light and temperature cues: multitasking receptors and transcriptional
403 integrators. *New Phytologist* 217(3): 1029-1034.

404 **Chen M, Schwab R, Chory J. 2003.** Characterization of the requirements for localization of
405 phytochrome B to nuclear bodies. *Proc Natl Acad Sci U S A* 100(24): 14493-14498.

406 **Clack T, Mathews S, Sharrock RA. 1994.** The phytochrome apoprotein family in *Arabidopsis*
407 is encoded by five genes: the sequences and expression of *PHYD* and *PHYE*. *Plant Mol*
408 *Biol* 25(3): 413-427.

409 **Clough SJ, Bent AF. 1998.** Floral dip: a simplified method for *Agrobacterium*-mediated
410 transformation of *Arabidopsis thaliana*. *Plant J* 16(6): 735-743.

411 **Darriba D, Taboada GL, Doallo R, Posada D. 2011.** ProtTest 3: fast selection of best-fit models
412 of protein evolution. *Bioinformatics* 27(8): 1164-1165.

413 **Darriba D, Taboada GL, Doallo R, Posada D. 2012.** jModelTest 2: more models, new heuristics
414 and parallel computing. *Nat Methods* 9(8): 772.

415 **Edgar RC. 2004.** MUSCLE: a multiple sequence alignment method with reduced time and space
416 complexity. *BMC Bioinformatics* 5: 113.

417 **Enderle B, Sheerin DJ, Paik I, Kathare PK, Schwenk P, Klose C, Ulbrich MH, Huq E,
418 Hiltbrunner A. 2017.** PCH1 and PCHL promote photomorphogenesis in plants by
419 controlling phytochrome B dark reversion. *Nat Commun* 8(1): 2221.

420 **Endo M, Nakamura S, Araki T, Mochizuki N, Nagatani A. 2005.** Phytochrome B in the
421 mesophyll delays flowering by suppressing *FLOWERING LOCUS T* expression in
422 *Arabidopsis* vascular bundles. *Plant Cell* 17(7): 1941-1952.

423 **Filiault DL, Wessinger CA, Dinneny JR, Lutes J, Borevitz JO, Weigel D, Chory J, Maloof
424 JN. 2008.** Amino acid polymorphisms in *Arabidopsis* phytochrome B cause differential
425 responses to light. *Proc Natl Acad Sci U S A* 105(8): 3157-3162.

426 **Franklin KA, Praekelt U, Stoddart WM, Billingham OE, Halliday KJ, Whitelam GC. 2003.**
427 Phytochromes B, D, and E act redundantly to control multiple physiological responses in
428 *Arabidopsis*. *Plant Physiology* 131(3): 1340-1346.

429 **Franklin KA, Quail PH. 2010.** Phytochrome functions in *Arabidopsis* development. *Journal of*
430 *Experimental Botany* 61(1): 11-24.

431 **Guindon S, Dufayard JF, Lefort V, Anisimova M, Hordijk W, Gascuel O. 2010.** New
432 algorithms and methods to estimate maximum-likelihood phylogenies: assessing the
433 performance of PhyML 3.0. *Systematic Biology* 59(3): 307-321.

434 **Huang H, McLoughlin KE, Sorkin ML, Burgie ES, Bindbeutel RK, Vierstra RD, Nusinow
435 DA. 2019.** PCH1 regulates light, temperature, and circadian signaling as a structural
436 component of phytochrome B-photobodies in *Arabidopsis*. *Proc Natl Acad Sci U S A*
437 116(17): 8603-8608.

438 **Ikeda H, Carlsen T, Fujii N, Brochmann C, Setoguchi H. 2012.** Pleistocene climatic
439 oscillations and the speciation history of an alpine endemic and a widespread arctic-alpine
440 plant. *New Phytologist* 194(2): 583-594.

441 **Ikeda H, Fujii N, Setoguchi H. 2009.** Molecular evolution of phytochromes in *Cardamine*
442 *nipponica* (Brassicaceae) suggests the involvement of *PHYE* in local adaptation. *Genetics*
443 182(2): 603-614.

444 **Ikeda H, Fujii N, Setoguchi H. 2011.** Molecular evolution of cryptochrome genes and the
445 evolutionary manner of photoreceptor genes in *Cardamine nipponica* (Brassicaceae). *J*
446 *Plant Res* 124(1): 85-92.

447 **Ikeda H, Senni K, Fujii N, Setoguchi H. 2008.** Consistent geographic structure among multiple
448 nuclear sequences and cpDNA polymorphisms of *Cardamine nipponica* Franch. et Savat.
449 (Brassicaceae). *Molecular Ecology* 17: 3178-3188.

450 **Ikeda H, Setoguchi H. 2010.** Natural selection on *PHYE* by latitude in the Japanese archipelago:
451 insight from locus specific phylogeographic structure in *Arctostaphylos nana* (Ericaceae).

- 452 *Molecular Ecology* **19**(13): 2779-2791.
- 453 **Ingvarsson PK, Garcia MV, Hall D, Luquez V, Jansson S. 2006.** Clinal variation in *phyB2*, a
454 candidate gene for day-length-induced growth cessation and bud set, across a latitudinal
455 gradient in European aspen (*Populus tremula*). *Genetics* **172**(3): 1845-1853.
- 456 **Ingvarsson PK, Garcia MV, Luquez V, Hall D, Jansson S. 2008.** Nucleotide polymorphism
457 and phenotypic associations within and around the *phytochrome B2* Locus in European
458 aspen (*Populus tremula*, Salicaceae). *Genetics* **178**(4): 2217-2226.
- 459 **Jiao Y, Lau OS, Deng XW. 2007.** Light-regulated transcriptional networks in higher plants. *Nat*
460 *Rev Genet* **8**(3): 217-230.
- 461 **Jung JH, Domijan M, Klose C, Biswas S, Ezer D, Gao M, Khattak AK, Box MS,
462 Charoensawan V, Cortijo S, et al. 2016.** Phytochromes function as thermosensors in
463 *Arabidopsis*. *Science* **354**(6314): 886-889.
- 464 **Kagale S, Robinson SJ, Nixon J, Xiao R, Huebert T, Condie J, Kessler D, Clarke WE, Edger
465 PP, Links MG, et al. 2014.** Polyploid evolution of the Brassicaceae during the Cenozoic
466 era. *Plant Cell* **26**(7): 2777-2791.
- 467 **Kong SG, Suzuki T, Tamura K, Mochizuki N, Hara-Nishimura I, Nagatani A. 2006.** Blue
468 light-induced association of phototropin 2 with the Golgi apparatus. *Plant J* **45**(6): 994-
469 1005.
- 470 **Kretsch T, Poppe C, Schafer E. 2000.** A new type of mutation in the plant photoreceptor
471 phytochrome B causes loss of photoreversibility and an extremely enhanced light
472 sensitivity. *Plant J* **22**(3): 177-186.
- 473 **Legris M, Klose C, Burgie ES, Rojas CC, Neme M, Hiltbrunner A, Wigge PA, Schafer E,
474 Vierstra RD, Casal JJ. 2016.** Phytochrome B integrates light and temperature signals in
475 *Arabidopsis*. *Science* **354**(6314): 897-900.
- 476 **Legris M, Nieto C, Sellaro R, Prat S, Casal JJ. 2017.** Perception and signalling of light and
477 temperature cues in plants. *Plant J* **90**(4): 683-697.
- 478 **Maloof JN, Borevitz JO, Dabi T, Lutes J, Nehring RB, Redfern JL, Trainer GT, Wilson JM,
479 Asami T, Berry CC, et al. 2001.** Natural variation in light sensitivity of *Arabidopsis*. *Nat*
480 *Genet* **29**(4): 441-446.
- 481 **Mathews S. 2010.** Evolutionary studies illuminate the structural-functional model of plant
482 phytochromes. *Plant Cell* **22**(1): 4-16.
- 483 **Molina-Contreras MJ, Paulisic S, Then C, Moreno-Romero J, Pastor-Andreu P, Morelli L,
484 Roig-Villanova I, Jenkins H, Hallab A, Gan X, et al. 2019.** Photoreceptor Activity
485 Contributes to Contrasting Responses to Shade in Cardamine and Arabidopsis Seedlings.
486 *Plant Cell* **31**(11): 2649-2663.
- 487 **Oka Y, Matsushita T, Mochizuki N, Quail PH, Nagatani A. 2008.** Mutant screen distinguishes
488 between residues necessary for light-signal perception and signal transfer by
489 phytochrome B. *PLoS Genet* **4**(8): e1000158.
- 490 **Oka Y, Matsushita T, Mochizuki N, Suzuki T, Tokutomi S, Nagatani A. 2004.** Functional
491 analysis of a 450-amino acid N-terminal fragment of phytochrome B in Arabidopsis.
492 *Plant Cell* **16**(8): 2104-2116.
- 493 **Reed JW, Nagpal P, Poole DS, Furuya M, Chory J. 1993.** Mutations in the gene for the red/far-
494 red light receptor phytochrome B alter cell elongation and physiological responses
495 throughout Arabidopsis development. *Plant Cell* **5**(2): 147-157.
- 496 **Ronquist F, Huelsenbeck JP. 2003.** MrBayes 3: Bayesian phylogenetic inference under mixed
497 models. *Bioinformatics* **19**(12): 1572-1574.
- 498 **Sharrock RA, Quail PH. 1989.** Novel phytochrome sequences in *Arabidopsis thaliana*: structure,
499 evolution, and differential expression of a plant regulatory photoreceptor family. *Genes*
500 *& Development* **3**(11): 1745-1757.
- 501 **Stephens M, Donnelly P. 2003.** A comparison of bayesian methods for haplotype reconstruction

502 from population genotype data. *American Journal of Human Genetics* **73**(5): 1162-1169.
503 **Sweere U, Eichenberg K, Lohrmann J, Mira-Rodado V, Baurle I, Kudla J, Nagy F, Schafer**
504 **E, Harter K. 2001.** Interaction of the response regulator ARR4 with phytochrome B in
505 modulating red light signaling. *Science* **294**(5544): 1108-1111.
506 **Toivainen T, Pyhajarvi T, Niittyvuopio A, Savolainen O. 2014.** A recent local sweep at the
507 *PHYA* locus in the Northern European Spiterstulen population of *Arabidopsis lyrata*.
508 *Molecular Ecology* **23**(5): 1040-1052.
509 **Van Buskirk EK, Reddy AK, Nagatani A, Chen M. 2014.** Photobody localization of
510 phytochrome B is tightly correlated with prolonged and light-dependent inhibition of
511 hypocotyl elongation in the dark. *Plant Physiology* **165**(2): 595-607.
512 **Yamaguchi R, Nakamura M, Mochizuki N, Kay SA, Nagatani A. 1999.** Light-dependent
513 translocation of a phytochrome B-GFP fusion protein to the nucleus in transgenic
514 *Arabidopsis*. *J Cell Biol* **145**(3): 437-445.
515 **Yang Z. 2007.** PAML 4: phylogenetic analysis by maximum likelihood. *Molecular Biology and*
516 *Evolution* **24**(8): 1586-1591.
517 **Yang Z, Nielsen R. 1998.** Synonymous and nonsynonymous rate variation in nuclear genes of
518 mammals. *J Mol Evol* **46**(4): 409-418.
519 **Zhang J, Stankey RJ, Vierstra RD. 2013.** Structure-guided engineering of plant phytochrome
520 B with altered photochemistry and light signaling. *Plant Physiology* **161**(3): 1445-1457.
521 **Supporting Information**
522 Additional Supporting Information may be found online in the Supporting Information
523 section at the end of the article.
524 **Fig. S1** Hypocotyl responses to various red light fluence rates in each accession of
525 *Cardamine bellidifolia* and *Cardamine nipponica*.
526 **Fig. S2** *PHYB* gene trees in Brassicaceae.
527 **Fig. S3** Schematic image of phytochrome domain and alignment of amino acid sequences
528 of CnPHYB and CbPHYB.
529 **Fig. S4** Red light responses in transgenic *Arabidopsis thaliana*.
530 **Fig. S5** Protein level of CbPHYB and CnPHYB in transgenic *Arabidopsis thaliana*.
531 **Fig. S6** In vitro thermal stability of Pfr of CbPHYB and CnPHYB.
532 **Fig. S7** Temperature dependent hypocotyl growth in transgenic *Arabidopsis thaliana*.
533 **Fig. S8** Mean monthly temperature in localities of *Cardamine bellidifolia* and *Cardamine*
534 *nipponica*.
535 **Table S1** Information of samples used in this study (separate Excel file).
536 **Table S2** Genetic diversity and divergence of phytochromes within and between
537 *Cardamine bellidifolia* and *Cardamine nipponica*.
538 **Table S3** Sources of outgroup sequences for phylogenetic analyses.
539

540 **Figure legends**

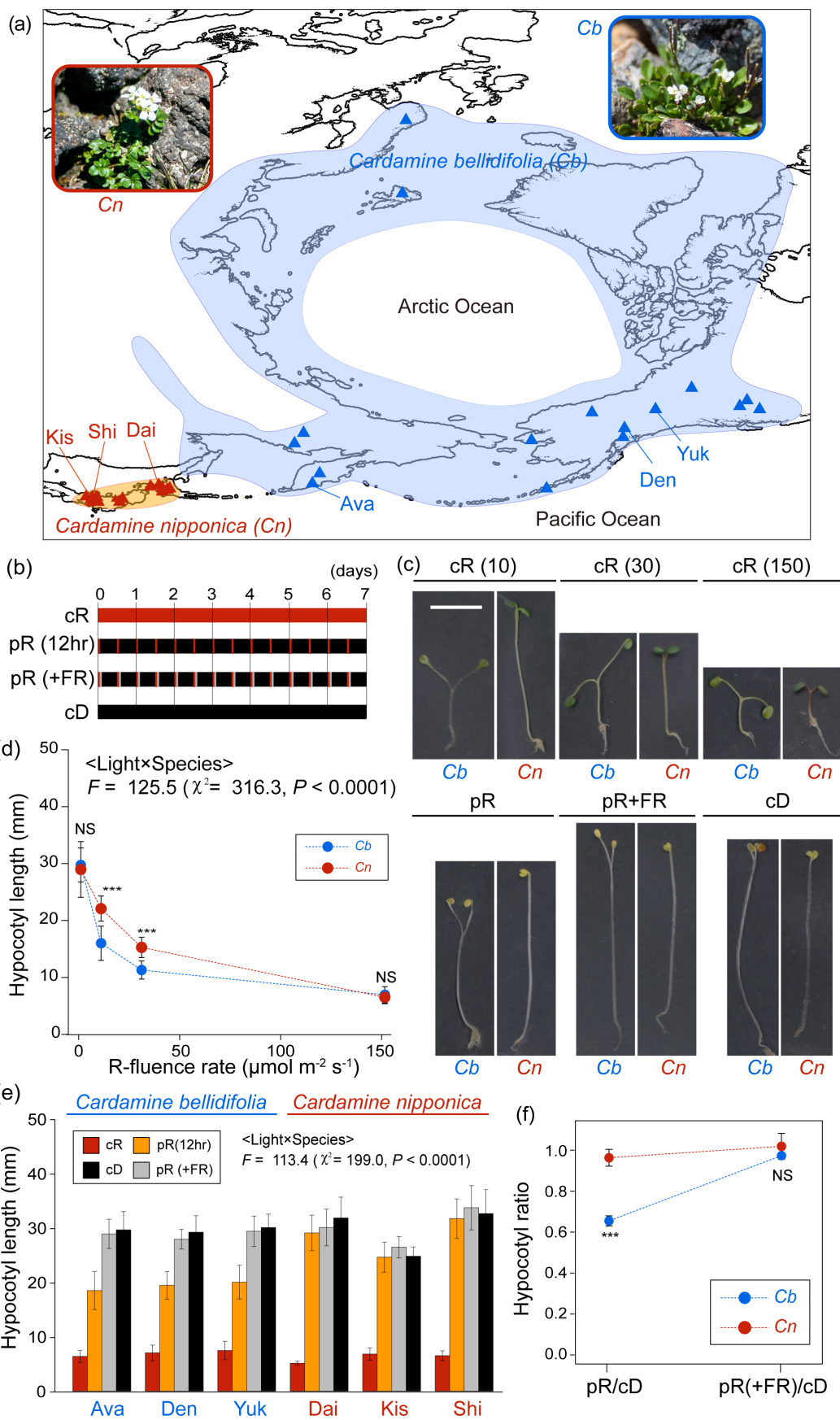
541 **Figure 1.** Red light sensitivity of *Cardamine bellidifolia* (*Cb*) and *Cardamine nipponica*
542 (*Cn*). (a) Sampling localities (triangles) and entire geographic range of the higher-latitude
543 species *Cb* (blue) and its lower-latitude sister species *Cn* (red). Localities of samples for
544 seedling assays are indicated by three-letter abbreviations. (b) Light conditions for
545 seedling assays. cR, continuous red light (R) light. pR, 15 min R pulses (ca. $150 \mu\text{mol m}^{-2} \text{sec}^{-1}$)
546 every 12 hr darkness. pR+FR, pR with 15 min far-red light pulse (ca. $100 \mu\text{mol m}^{-2} \text{sec}^{-1}$)
547 immediately after R pulses. cD, continuous darkness. Seedling assay was
548 performed for seven days at 22 °C. (c) Representative seedlings grown in the seedling
549 assay. The number in parentheses after cR is R fluence rate (ca. 10, 30 and $150 \mu\text{mol m}^{-2} \text{sec}^{-1}$).
550 Scale bar = 10 mm. (d) Hypocotyl growth responses to cR with different R fluence
551 rates for seven days at 22 °C. Data are the means \pm SD ($n \geq 70$). *** and NS, significant
552 ($P < 0.0001$) and nonsignificant result, respectively, evaluated by generalized linear
553 mixed model. (e) Hypocotyl growth responses of each accession to cR (ca. $150 \mu\text{mol m}^{-2} \text{sec}^{-1}$),
554 pR, pR+FR and cD for seven days at 22 °C. Data are the means \pm SD ($n \geq 10$) (f)
555 Relative hypocotyl length in pR and pR+FR compared to the length in cD. Data are the
556 mean of mean ratios of each accession \pm SD.

557 **Figure 2.** Molecular evolution of phytochrome genes of *Cardamine bellidifolia* and
558 *Cardamine nipponica*. (a) Numbers of synonymous and nonsynonymous substitutions are
559 shown for fixed differences between *C. bellidifolia* and *C. nipponica* (interspecific) and
560 polymorphisms within both species (intraspecific). *, significant results of the McDonald-
561 Kreitman test ($P < 0.05$). (b) Maximum likelihood tree of *PHYB* for the Brassicaceae
562 based on amino acid (AA) sequences. ●, nodes supported both by AA and nucleotide
563 (DNA) sequences (bootstrap > 90 and posterior probability > 0.95). ○, nodes supported
564 solely by DNA sequence data. Evolutionary patterns Results of molecular evolution
565 implemented by PAML are shown in the box. (c) Fixed differences in amino acid residues
566 in *PHYB* between *C. bellidifolia* and *C. nipponica*. Amino acid residues of outgroups at
567 each polymorphic site are also included.

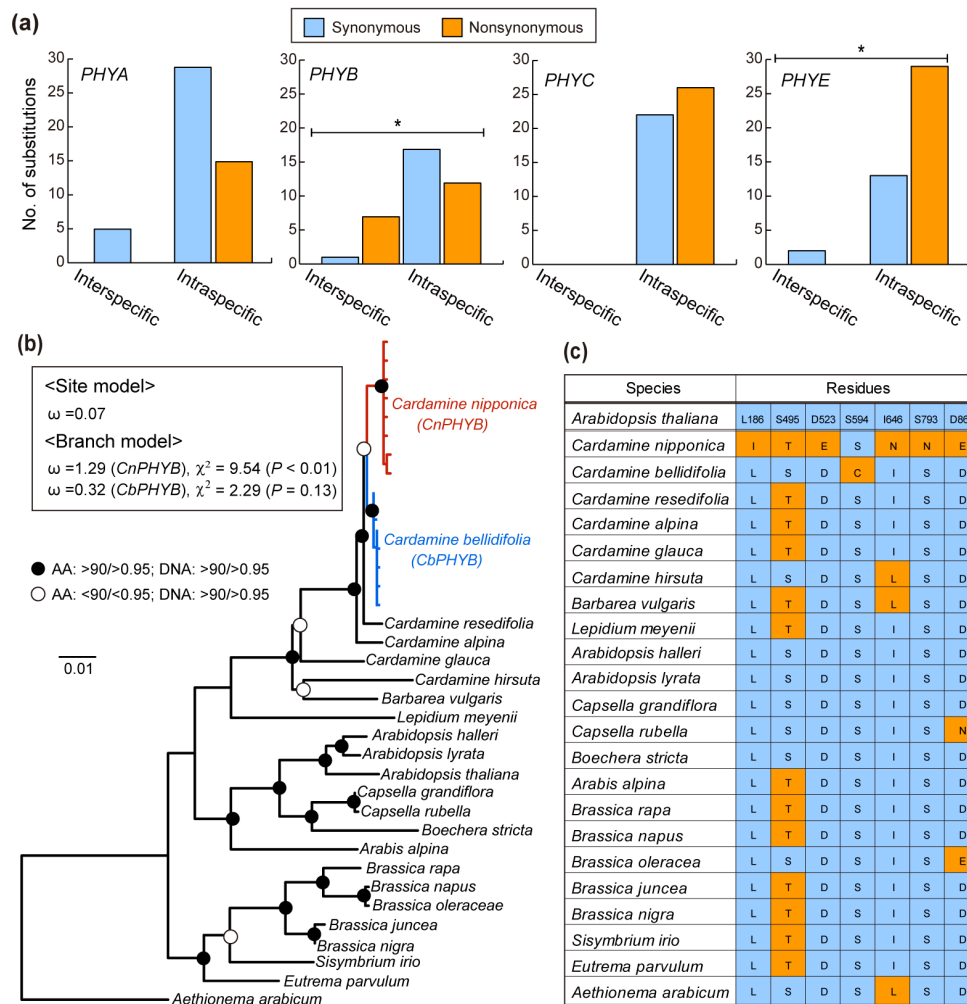
568

569 **Figure 3.** Red light sensitivity conferred by *PHYB* of *Cardamine bellidifolia* (*Cb*) and
570 *Cardamine nipponica* (*Cn*) in *Arabidopsis thaliana*. (a) Light conditions used for seedling
571 assays. Seedlings were grown in continuous red light (cR; ca. 30 $\mu\text{mol m}^{-2} \text{sec}^{-1}$), 15 min
572 red light pulses (ca. 30 $\mu\text{mol m}^{-2} \text{sec}^{-1}$) every 12 hr darkness (pR), 15 min far-red light
573 pulses (ca. 100 $\mu\text{mol m}^{-2} \text{sec}^{-1}$) after pulse red [pR (+FR)] and continuous darkness (cD)
574 for five days at 22 °C. (b) Mean hypocotyl length (mm) of $35S_{\text{pro}}::\text{PHYB-GFP}$ transgenic
575 *A. thaliana* (*phyB-5* mutant) grown in cR, pR, pR (+FR) and cD ($n \geq 25$). Three
576 independent lines of each transgenic line were analysed. Error bars indicate standard
577 deviation. (c) Relative hypocotyl length in cR, pR and pR (+FR) compared to the length
578 in cD. Blue and red line indicates transgenic lines with *CbPHYB* and *CnPHYB*,
579 respectively. Data are the mean of mean ratios of each transgenic line \pm SD. *** and NS,
580 significant ($P < 0.001$) and nonsignificant result, respectively, evaluated by generalized
581 linear mixed model. (d) Area of phyB nuclear bodies (NBs) in two-day old seedlings of
582 transgenics before (0 hr) and after (12 hr) 12 hr darkness. The box represents interquartile,
583 the bold black line in the box is the median, the whiskers indicate values greater than the
584 interquartile excluding outliers, which are represented by circles. *CbPHYB* and *CnPHYB*
585 includes three independent transgenic lines ($n \geq 25$ for each line). (e) Representative
586 confocal images of GFP signals from NBs in nucleus of hypocotyl epidermal cells in two-
587 day old seedlings . Scale bar = 2.0 μm .

588 **Figure 4.** Temperature dependent seedling growth conferred by *PHYB* of *Cardamine*
589 *bellidifolia* (*Cb*) and *Cardamine nipponica* (*Cn*) in *Arabidopsis thaliana*. (a) Boxplot of
590 hypocotyl length (mm) of $35S_{\text{pro}}::\text{PHYB-GFP}$ transgenic *A. thaliana* (*phyB-5* mutant)
591 grown at 16, 22, and 28 °C in continuous red light (cR; ca. 30 $\mu\text{mol m}^{-2} \text{sec}^{-1}$), 15 min red
592 light pulses (ca. 30 $\mu\text{mol m}^{-2} \text{sec}^{-1}$) every 12 hr darkness (pR) and continuous dark (cD)
593 for five days. The box represents interquartile, the bold black line in the box is the median,
594 the whiskers indicate values greater than the interquartile excluding outliers, which are
595 represented by circles. *CbPHYB* and *CnPHYB* includes three independent transgenic lines
596 ($n \geq 25$ for each line). (b) Relative hypocotyl length in cR and pR compared to the length
597 in cD. Data are the mean of mean ratios of each transgenic line \pm SD. *** and NS,
598 significant ($P < 0.001$) and nonsignificant result, respectively, evaluated by generalized
599 linear mixed model.



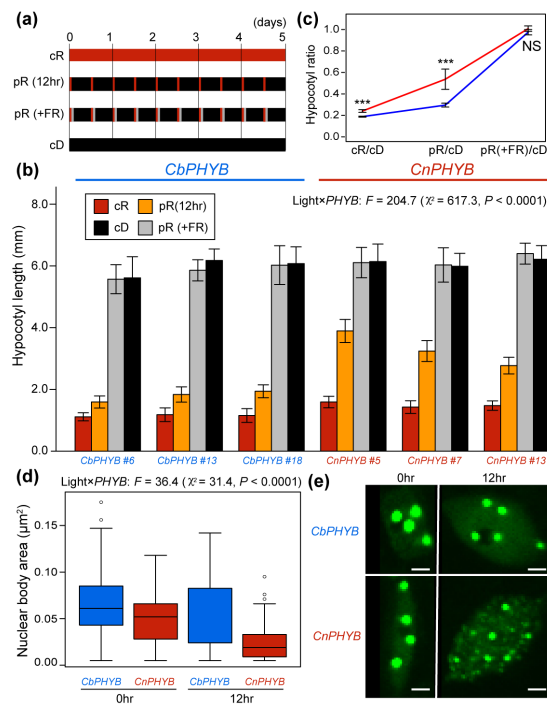
601 **Figure 1.** Red light sensitivity of *Cardamine bellidifolia* (*Cb*) and *Cardamine nipponica*
602 (*Cn*). (a) Sampling localities (triangles) and entire geographic range of the higher-latitude
603 species *Cb* (blue) and its lower-latitude sister species *Cn* (red). Localities of samples for
604 seedling assays are indicated by three-letter abbreviations. (b) Light conditions for
605 seedling assays. cR, continuous red light (R) light. pR, 15 min R pulses (ca. $150 \mu\text{mol m}^{-2} \text{sec}^{-1}$)
606 every 12 hr darkness. pR+FR, pR with 15 min far-red light pulse (ca. $100 \mu\text{mol m}^{-2} \text{sec}^{-1}$)
607 immediately after R pulses. cD, continuous darkness. Seedling assay was
608 performed for seven days at 22 °C. (c) Representative seedlings grown in the seedling
609 assay. The number in parentheses after cR is R fluence rate (ca. 10, 30 and $150 \mu\text{mol m}^{-2}$
610 sec^{-1}). Scale bar = 10 mm. (d) Hypocotyl growth responses to cR with different R fluence
611 rates for seven days at 22 °C. Data are the means \pm SD ($n \geq 70$). *** and NS, significant
612 ($P < 0.0001$) and nonsignificant result, respectively, evaluated by generalized linear
613 mixed model. (e) Hypocotyl growth responses of each accession to cR (ca. $150 \mu\text{mol m}^{-2} \text{sec}^{-1}$)
614 sec^{-1}), pR, pR+FR and cD for seven days at 22 °C. Data are the means \pm SD ($n \geq 10$) (f)
615 Relative hypocotyl length in pR and pR+FR compared to the length in cD. Data are the
616 mean of mean ratios of each accession \pm SD.
617



618

619 **Figure 2.** Molecular evolution of phytochrome genes of *Cardamine bellidifolia* and
620 *Cardamine nipponica*. (a) Numbers of synonymous and nonsynonymous substitutions are
621 shown for fixed differences between *C. bellidifolia* and *C. nipponica* (interspecific) and
622 polymorphisms within both species (intraspecific). *, significant results of the McDonald-
623 Kreitman test ($P < 0.05$). (b) Maximum likelihood tree of *PHYB* for the Brassicaceae
624 based on amino acid (AA) sequences. ●, nodes supported both by AA and nucleotide
625 (DNA) sequences (bootstrap > 90 and posterior probability > 0.95). ○, nodes supported
626 solely by DNA sequence data. Evolutionary patterns Results of molecular evolution
627 implemented by PAML are shown in the box. (c) Fixed differences in amino acid residues
628 in *PHYB* between *C. bellidifolia* and *C. nipponica*. Amino acid residues of outgroups at
629 each polymorphic site are also included.

630



631

632

633

634

635

636

637

638

639

640

641

642

643

644

645

646

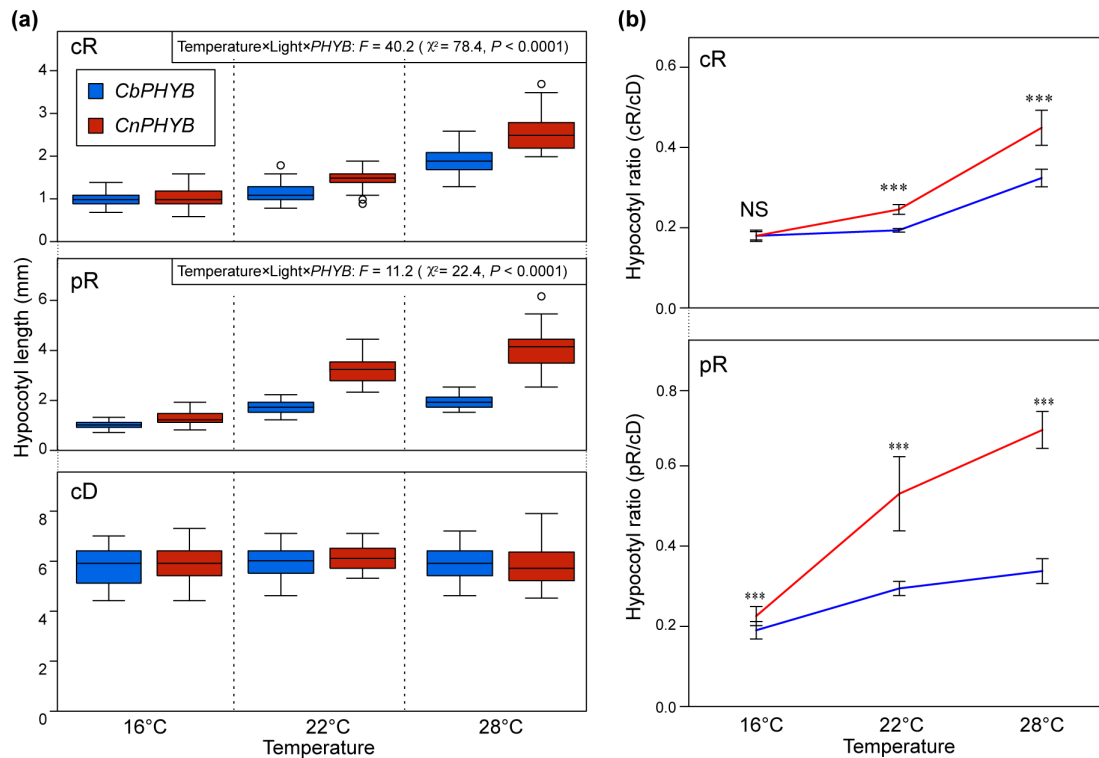
647

648

649

650

Figure 3. Red light sensitivity conferred by *PHYB* of *Cardamine bellidifolia* (*Cb*) and *Cardamine nipponica* (*Cn*) in *Arabidopsis thaliana*. (a) Light conditions used for seedling assays. Seedlings were grown in continuous red light (cR; ca. $30 \mu\text{mol m}^{-2} \text{sec}^{-1}$), 15 min red light pulses (ca. $30 \mu\text{mol m}^{-2} \text{sec}^{-1}$) every 12 hr darkness (pR), 15 min far-red light pulses (ca. $100 \mu\text{mol m}^{-2} \text{sec}^{-1}$) after pulse red [pR (+FR)] and continuous darkness (cD) for five days at 22°C . (b) Mean hypocotyl length (mm) of $35S_{\text{pro}}::\text{PHYB-GFP}$ transgenic *A. thaliana* (*phyB-5* mutant) grown in cR, pR, pR (+FR) and cD ($n \geq 25$). Three independent lines of each transgenic line were analysed. Error bars indicate standard deviation. (c) Relative hypocotyl length in cR, pR and pR (+FR) compared to the length in cD. Blue and red line indicates transgenic lines with *CbPHYB* and *CnPHYB*, respectively. Data are the mean of mean ratios of each transgenic line \pm SD. *** and NS, significant ($P < 0.001$) and nonsignificant result, respectively, evaluated by generalized linear mixed model. (d) Area of phyB nuclear bodies (NBs) in two-day old seedlings of transgenics before (0 hr) and after (12 hr) 12 hr darkness. The box represents interquartile, the bold black line in the box is the median, the whiskers indicate values greater than the interquartile excluding outliers, which are represented by circles. *CbPHYB* and *CnPHYB* includes three independent transgenic lines ($n \geq 25$ for each line). (e) Representative confocal images of GFP signals from NBs in nucleus of hypocotyl epidermal cells in two-day old seedlings. Scale bar = $2.0 \mu\text{m}$.



651

652 **Figure 4.** Temperature dependent seedling growth conferred by *PHYB* of *Cardamine*
 653 *bellidifolia* (*Cb*) and *Cardamine nipponica* (*Cn*) in *Arabidopsis thaliana*. (a) Boxplot of
 654 hypocotyl length (mm) of $35S_{pro}::PHYB-GFP$ transgenic *A. thaliana* (*phyB-5* mutant)
 655 grown at 16, 22, and 28°C in continuous red light (cR; ca. $30 \mu\text{mol m}^{-2} \text{sec}^{-1}$), 15 min red
 656 light pulses (ca. $30 \mu\text{mol m}^{-2} \text{sec}^{-1}$) every 12 hr darkness (pR) and continuous dark (cD)
 657 for five days. The box represents interquartile, the bold black line in the box is the median,
 658 the whiskers indicate values greater than the interquartile excluding outliers, which are
 659 represented by circles. *CbPHYB* and *CnPHYB* includes three independent transgenic lines
 660 ($n \geq 25$ for each line). (b) Relative hypocotyl length in cR and pR compared to the length
 661 in cD. Data are the mean of mean ratios of each transgenic line \pm SD. *** and NS,
 662 significant ($P < 0.001$) and nonsignificant result, respectively, evaluated by generalized
 663 linear mixed model.